Supporting Information

Electrodeposited nickel-sulfide films as competent hydrogen evolution catalysts in neutral water

Nan Jiang,[a] Lia Bogoev,[a] Marina Popova,[a] Sheraz Gul,[b] Junko Yano[b] and Yujie Sun*[a]

[a] Department of Chemistry and Biochemistry, Utah State University, Logan, Utah 84322, United States; [b] Physical Biosciences Division, Lawrence Berkeley National Laboratory, Berkeley, California 94720, United States.
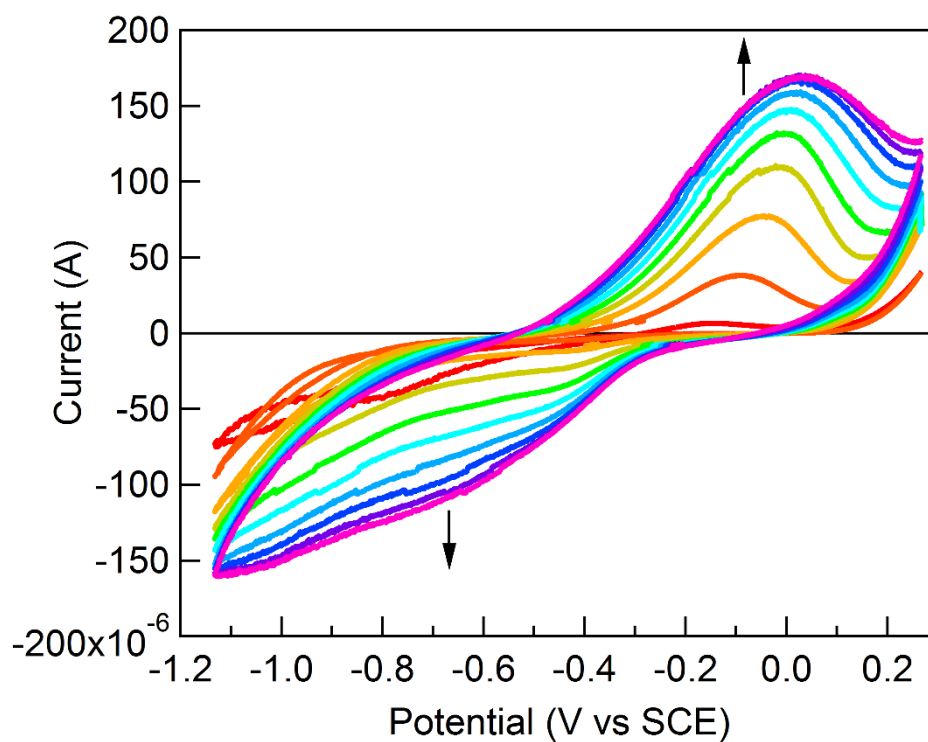
Figure S1. A typical potentiodynamic deposition for preparation of Ni-S films on FTO (scan rate: 5 mV/s).
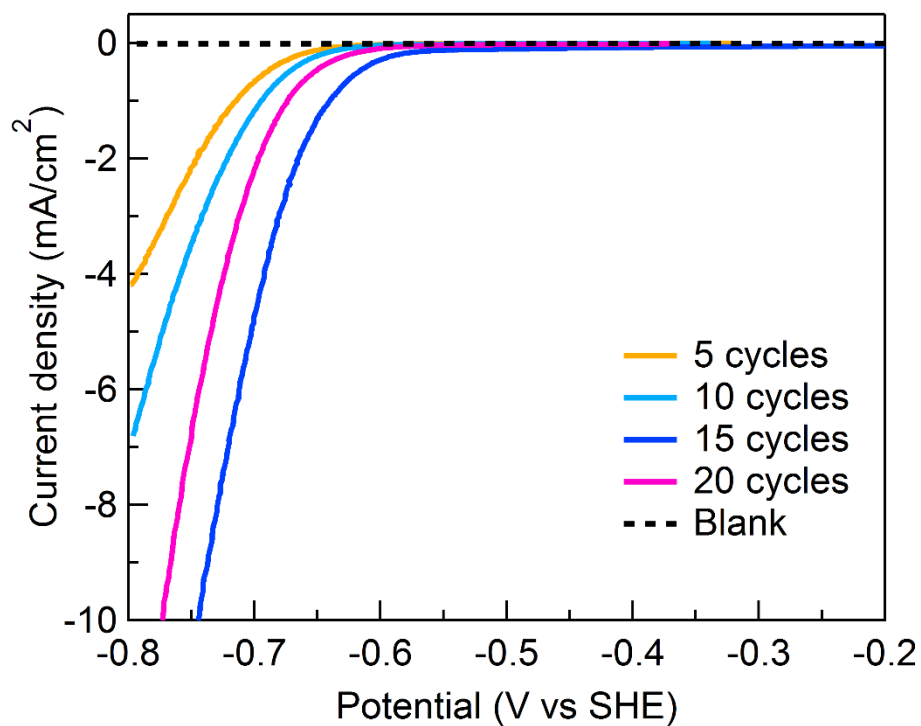
Figure S2. Cathodic scans of Ni-S/FTO samples prepared with 5, 10, 15, and 20 deposition cycles in 1.0 M phosphate buffer of pH 7, where the one of 15 deposition cycles exhibits the highest activity for hydrogen evolution.
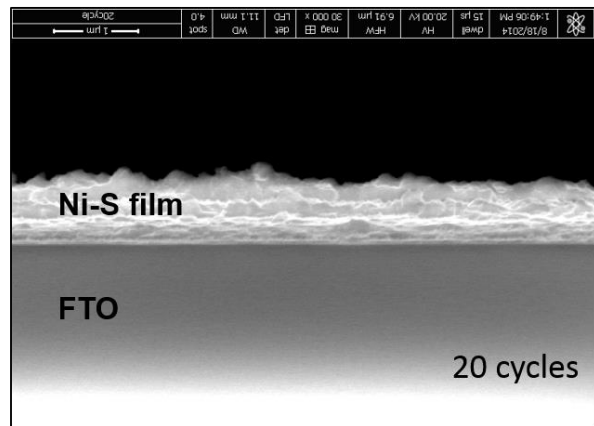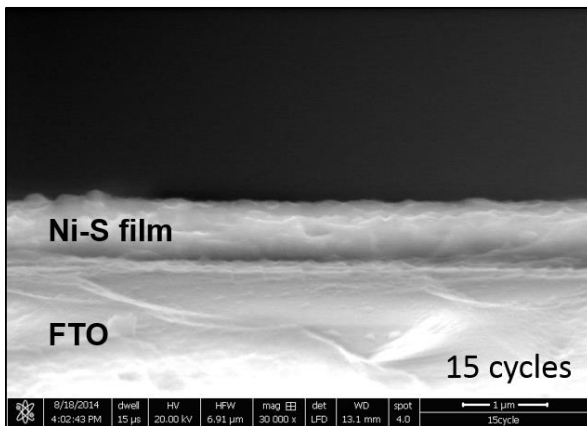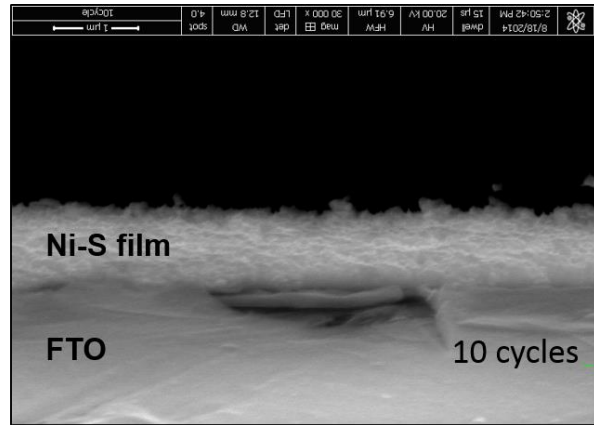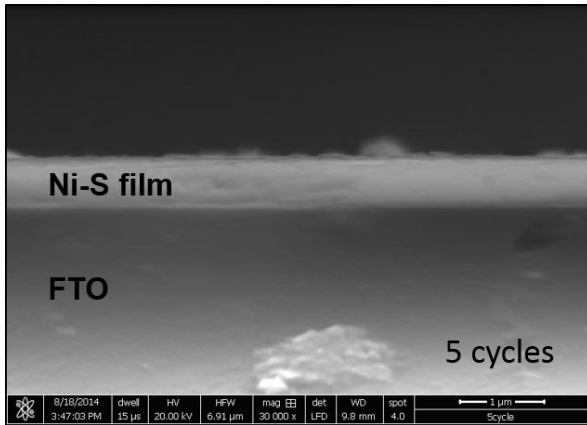
Figure S3. Cross section SEM images of four deposited Ni-S film on FTO prepared by 5, 10, 15, and 20 cycles, respectively.
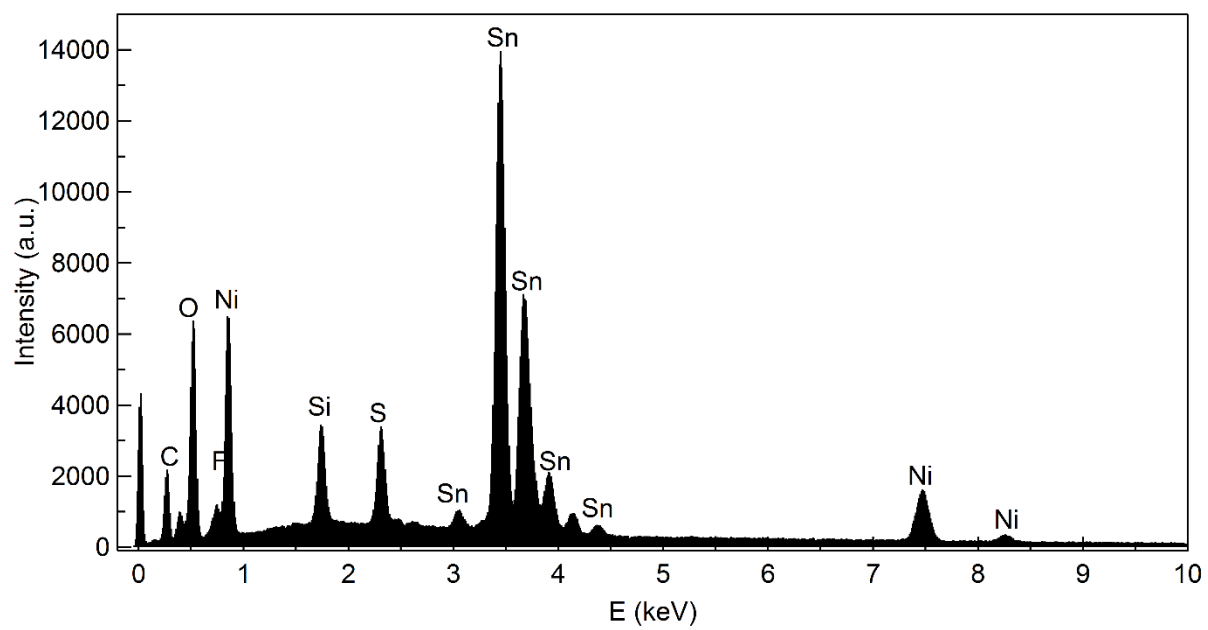
Figure S4. EDS of the Ni-S film on FTO.
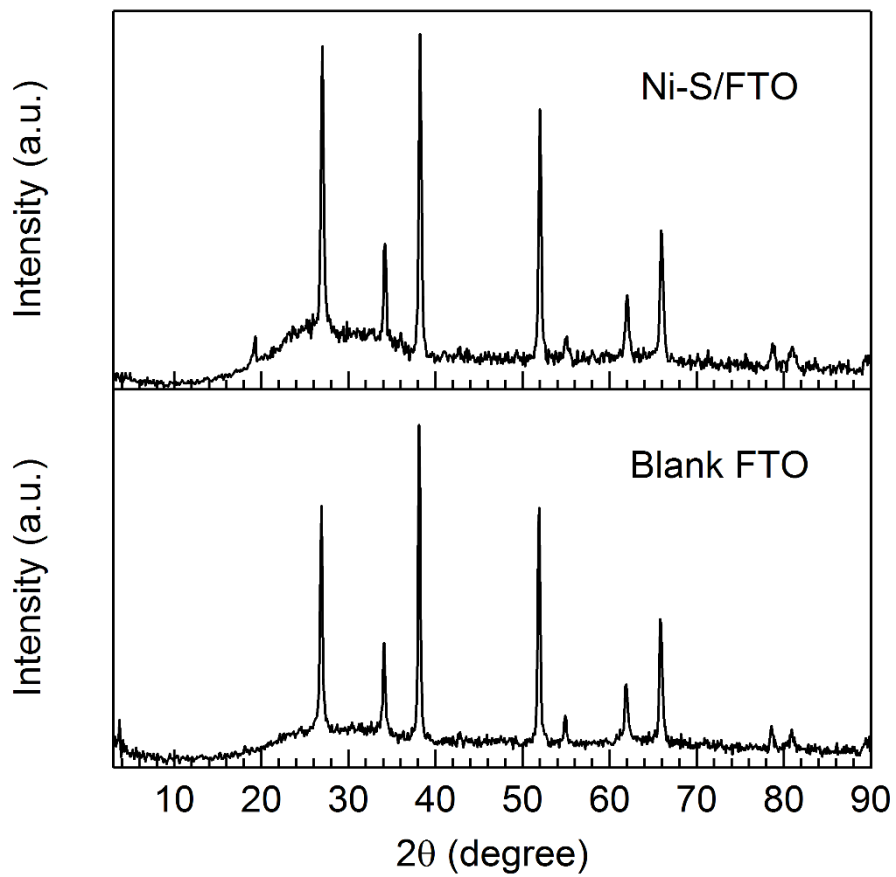
Figure S5. XRD of Ni-S/FTO and blank FTO.

Table S1. ICP-OES data of four Ni-S/FTO samples.

Sample	Area (cm^2)	Ni (μmol)	S (μmol)	[Ni] (μg/cm^2)	Ni/S
1	0.385	1.0005	0.7884	79.89	1.25
2	0.735	1.0601	0.6443	82.96	1.65
3	0.750	1.0165	0.5443	79.55	1.85
4	0.750	0.5479	0.3845	83.61	1.4
			Average	**81.50**	**1.55**

Table S2. Comparison of selected state-of-the-art solid-state HER electrocatalysts in **neutral** media.

Catalyst	Loading	Electrolyte	k^a (mV/dec)	$\eta_1{}^b$ (mV)	$\eta_{10}{}^b$ (mV)	Electrolysis	Faradaic Efficiency	Reference
Ni-S film	**Ni = 81.5 μg/cm^2**	**1.0 M KPi**	**77**	**227**	**330**	**100 h at η = 245 mV**	**100%**	**This work**
H$_2$-NiCat film	-	0.1 M NaBi (pH = 9.2)	226	~250	>600	24 h at η = 452 mV	100%	*J. Phys. Chem. C*, 2014, **118**, 4578.
MoS$_2$ film	-	KPi	86	~240	>450	-	-	*Chem. Sci.*, **2011**, 2, 1262.
H$_2$-CoCat	Co = 58.9 μg/cm^2	0.5 M KPi	140	~ 325	-	-	100%	*Nat. Mater.*, **2012**, *11*, 802.
M-MoS$_2{}^c$	Mo = 14 μg/cm^2	KPi	87-96	200–300	-	-	-	*Chem. Sci.*, **2012**, 3, 2515.
Cu$_2$MoS$_4$	41.6 μg/cm^2	0.1 M KPi	95	~ 200	~ 350	2 h at η = 300 mV	100%	*Energy Environ. Sci.*, **2012**, 5, 8912.
Co-S film	Co = 79.6 μg/cm^2	1.0 M KPi	93	56	166	40 h at η = 187 mV	100%	*J. Am. Chem. Soc.*, **2013**, 135, 17699
FeS	-	1.0 M KPi	150	~ 650	-	120 h at η = 350 mV	100%	*ACS Catalysis* **2014**, 681.
Co-NRCNT^d	280 μg/cm^2	0.1 M KPi	-	330	540	10 h at η = 330 mV	100%	*Angew. Chem. Int. Ed.*, **2014**, *53*, 4372.
CoP/CC^e	0.92 mg/cm^2	1.0 M KPi	93	~ 60	-	-	100%	*J. Am. Chem. Soc.*, **2014**, *136*, 7587-7590.

^{a}Tafel slope. ^{b}Overpotentials required to reach current densities of 1 or 10 mA/cm^2. ^{c}M: Mn, Fe, Co, Ni, Cu, and Zn. ^{d}NRCNT: nitrogen-rich carbon nanotube. ^{e}CC: carbon cloth.

Table S3. Comparison of selected state-of-the-art solid-state HER electrocatalysts in **strong acidic** aqueous media.

Catalyst	Loading	$[H_2SO_4]$ (M)	k^{a} (mV/dec)	η_1^{b} (mV)	η_{10}^{b} (mV)	η_{20}^{b} (mV)	Electrolysis	Reference
Ni-S film	**Ni = 81.5 μg/cm^2**	**0.5**	**52**	**150**	**213**	**243**	**1.5 h at η = 150 mV**	**This work**
MoS$_2$ film	-	1	40	~170	~215	~235	1 h at η = 200 mV	*Chem. Sci.* **2011**, *2*, 1262.
MoS$_2$/RGO	0.28 mg/cm^2	0.5	41	-	-	170	-	*J. Am. Chem. Soc.,* **2011**, *133*, 7296.
M-MoS$_2^{c}$	Mo = 14 μg/cm^2	1	39-43	-	180–210	200–230	1 h at η = 200 mV	*Chem. Sci.,* **2012**, *3*, 2515.
Cu$_2$MoS$_4$s	0.0416 mg/cm^2	0.5	95	~ 200	~ 300	-	-	*Energy Environ. Sci.,* **2012**, *5*, 8912.
MoB	2.5 mg/cm^2	1	55	-	~ 212	~ 227	48 h at η = 195 mV	*Angew. Chem. Int. Ed.,* **2012**, *51*, 12703.
Mo$_2$C	1.4 mg/cm^2	1	56	-	~ 210	~ 225	48 h at η = 195 mV	*Angew. Chem. Int. Ed.,* **2012**, *51*, 12703.
MoSoy	Mo$_2$C = 1.4 mg/cm^2	0.1 M HClO$_4$	66.4	-	177	-	500 h at i = 10 mA/cm^2	*Energy Environ. Sci.* **2013**, *6*, 1818.
FeP	-	0.5	67	-	~ 220	~ 300	-	*Chem. Commun.* **2013**, *49*, 6656.
Ni$_2$P crystal	1 mg/cm^2	0.5	81	-	-	130	-	*J. Am. Chem. Soc.,* **2013**, *135*, 9267.
Co-S film	Co = 79.6 μg/cm^2	0.5	56	60	156	220	-	*J. Am. Chem. Soc.,* **2013**, *135*, 17699
Mo$_2$C	0.21 mg/cm^2	0.5	53	-	~ 125	~ 150	25 h at η = 130 mV	*Energy Environ. Sci.* **2014**, *7*, 387.
Co-NRCNT^{d}	0.28 mg/cm^2	0.5	69	140	260	-	10 h at η = 140 mV	*Angew. Chem. Int. Ed.,* **2014**, *53*, 4372.
CoSe$_2$/CP^{e}	2.8 mg/cm^2	0.5	40	-	139	150	60 h at η = 155 mV	*J. Am. Chem. Soc.,* **2014**, *136*, 4897.
Ni$_2$P	0.38 mg/cm^2	1	66 (87)	-	~120	140	48 h at η = 170 mV	*Phys. Chem. Chem. Phys.,* **2014**, *16*, 5917.
CoP	0.9 mg/cm^2	0.5	50	-	-	95	24 h at i = 20 mA/cm^2	*Angew. Chem. Int. Ed.,* **2014**, *53*, 5427-5430.
CoP/CC^{f}	0.92 mg/cm^2	0.5	51	-	67	100	22.2 h at η = 200 mV	*J. Am. Chem. Soc.,* **2014**, 136, 7587-7590.
CoP/CNT	0.285 mg/cm^2	0.5	54	-	122	~155	18 h at η = 122 mV	*Angew. Chem. Int. Ed.* **2014**, 53, 6710-6714.

[a]Tafel slope. [b]Overpotentials required to reach current densities of 1, 10, or 20 mA/cm^2. [c]M: Mn, Fe, Co, Ni, Cu, and Zn. [d]NRCNT: nitrogen-rich carbon nanotube. [e]CP: carbon fiber paper. [f]CC: carbon cloth.
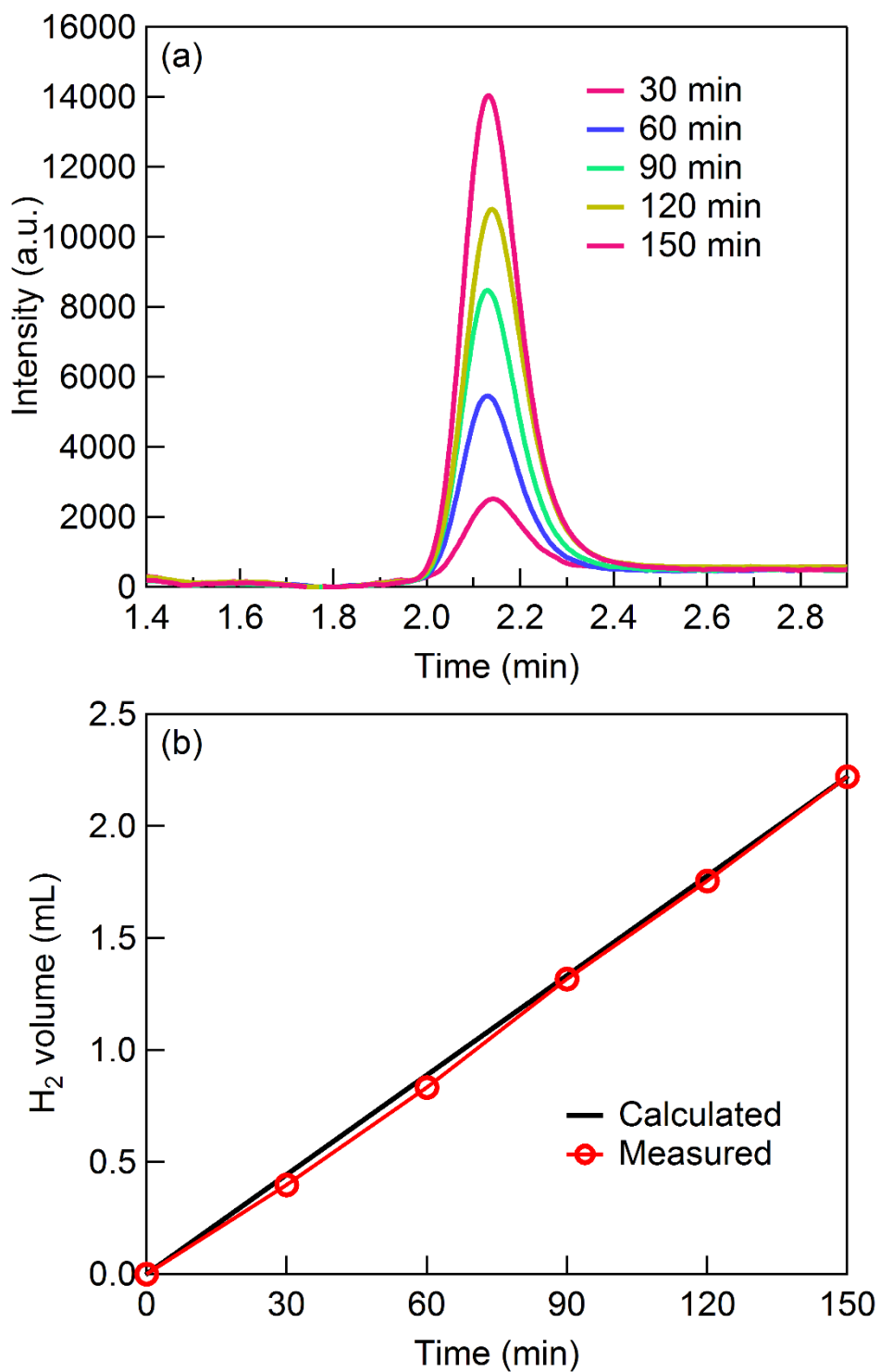
Figure S6. (a) Gas chromatograms of generated hydrogen during a 2.5-h chronopotentiometry experiment of Ni-S/FTO at 2 mA in pH 7 phosphate buffer. (b) Overlay of the measured hydrogen volume (red) from gas chromatography every 30 min and the calculated hydrogen volume (black) based on the assumption that all the passed charge during the electrolysis were used to produce hydrogen.
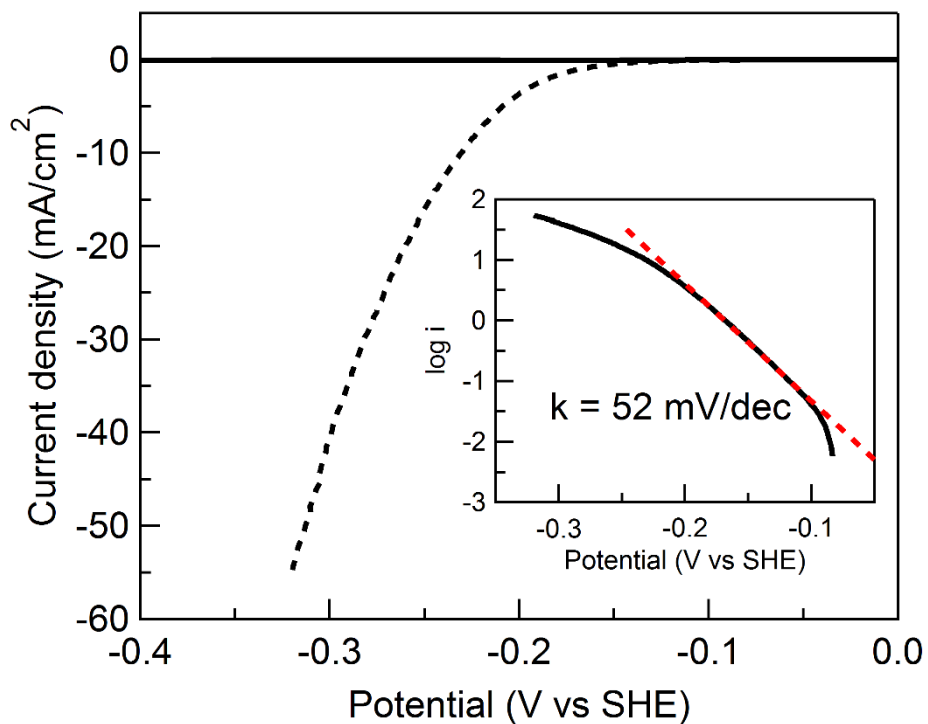
Figure S7. Polarization of Ni-S/FTO in 0.5 M H$_2$SO$_4$ at scan rate of 2 mV/s. Inset shows the corresponding Tafel plot and slope.
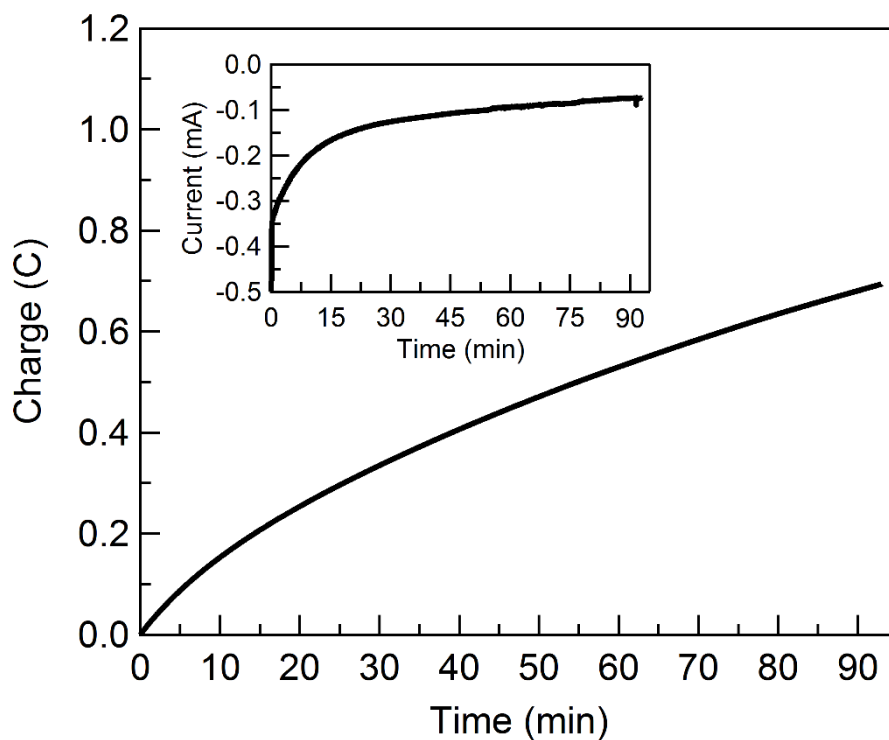
Figure S8. Controlled potential electrolysis shows the accumulated charge versus time for Ni-S/FTO in 0.5 M H$_2$SO$_4$ with an applied potential of −0.168 V vs SHE. Inset shows current versus time during the electrolysis.
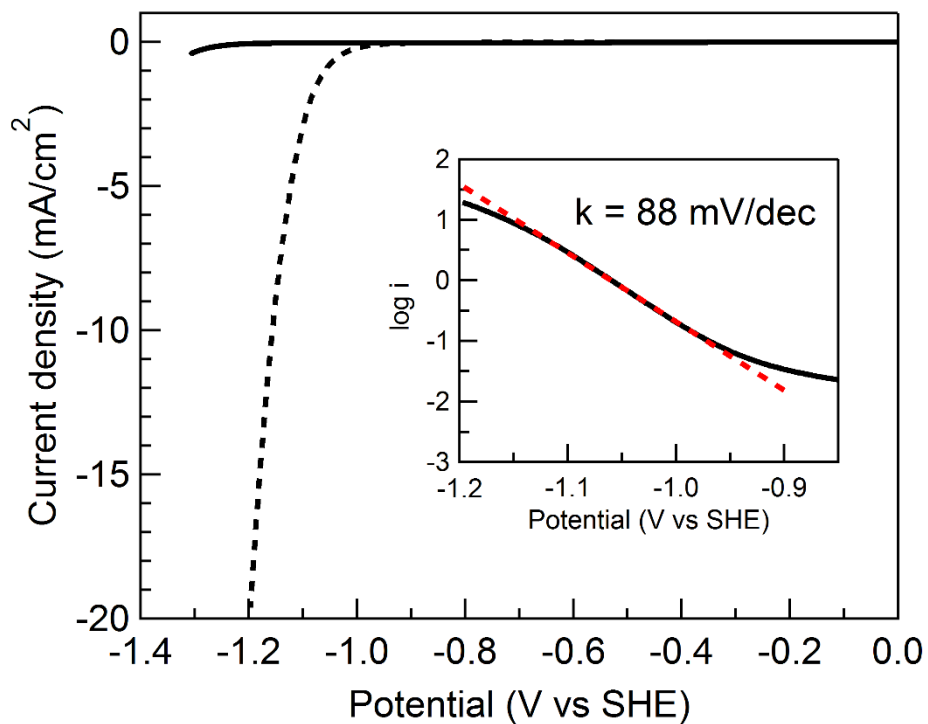
Figure S9. Polarization of Ni-S/FTO in 1.0 M KOH at scan rate of 2 mV/s. Inset shows the corresponding Tafel plot and slope.
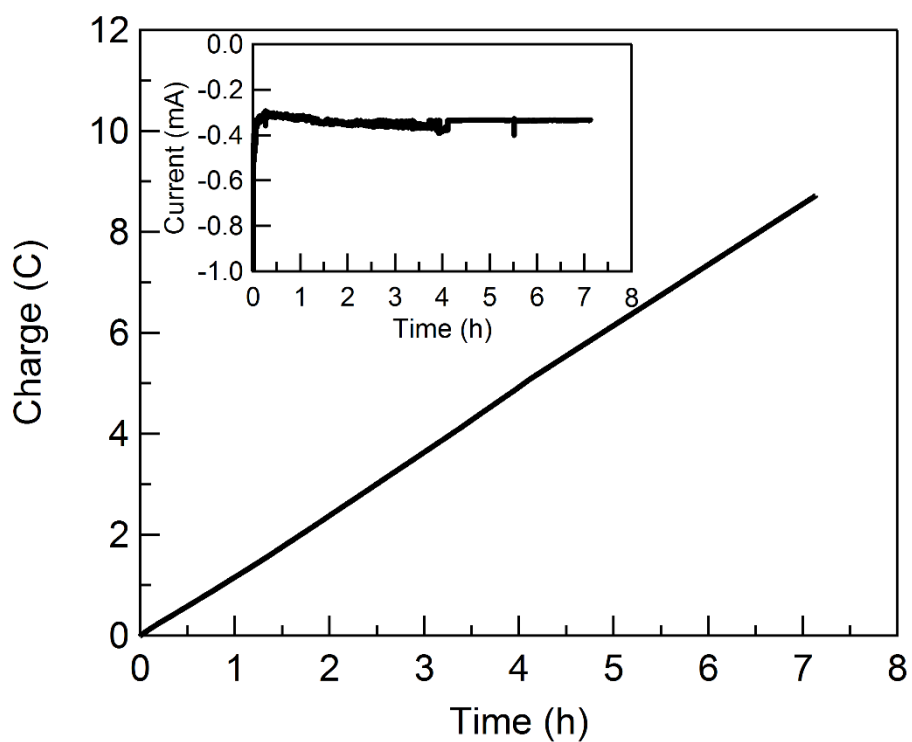
Figure S10. Controlled potential electrolysis shows the accumulated charge versus time for Ni-S/FTO in 1.0 M KOH at an applied potential of −1.05 V vs SHE. Inset shows current versus time during the electrolysis.
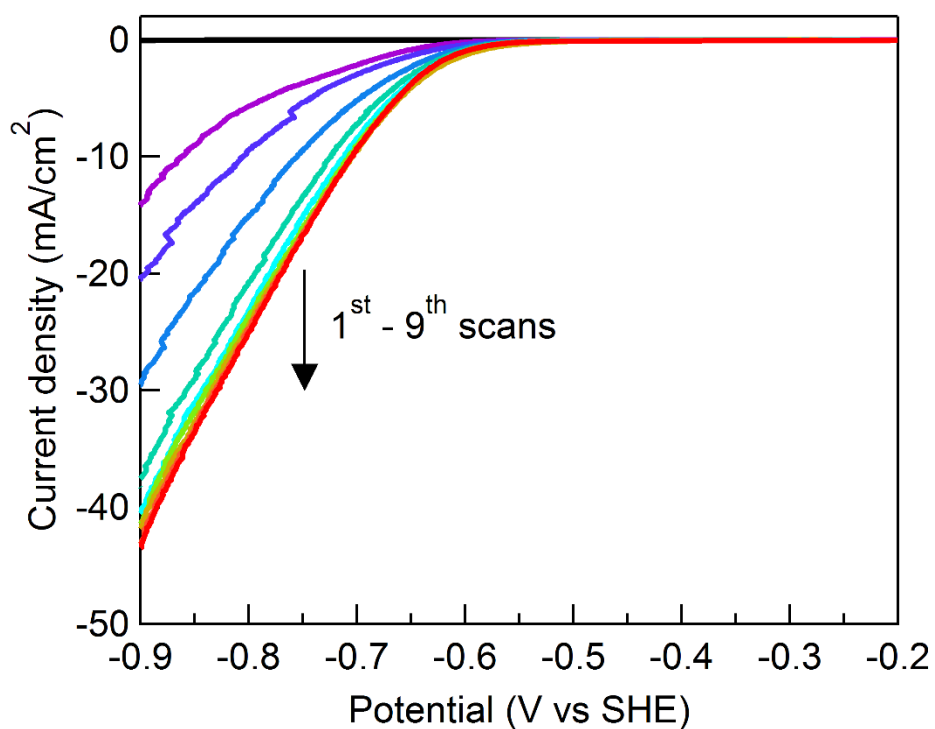
Figure S11. Consecutive nine polarizations of Ni-S/FTO in 1.0 M phosphate buffer at pH 7 (scan rate: 2 mV/s). The black curve is for a blank FTO electrode under the same condition.
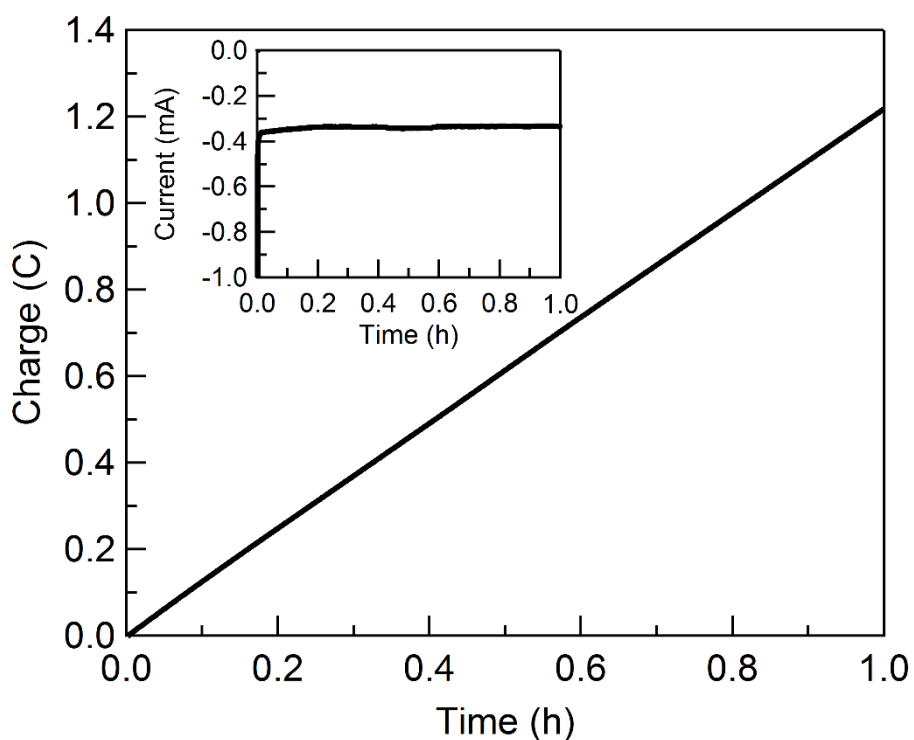
Figure S12. Accumulated change over time during the controlled potential electrolysis of Ni-S/FTO at −0.689 V vs SHE in pH 7 phosphate buffer. Inset shows the current versus time.
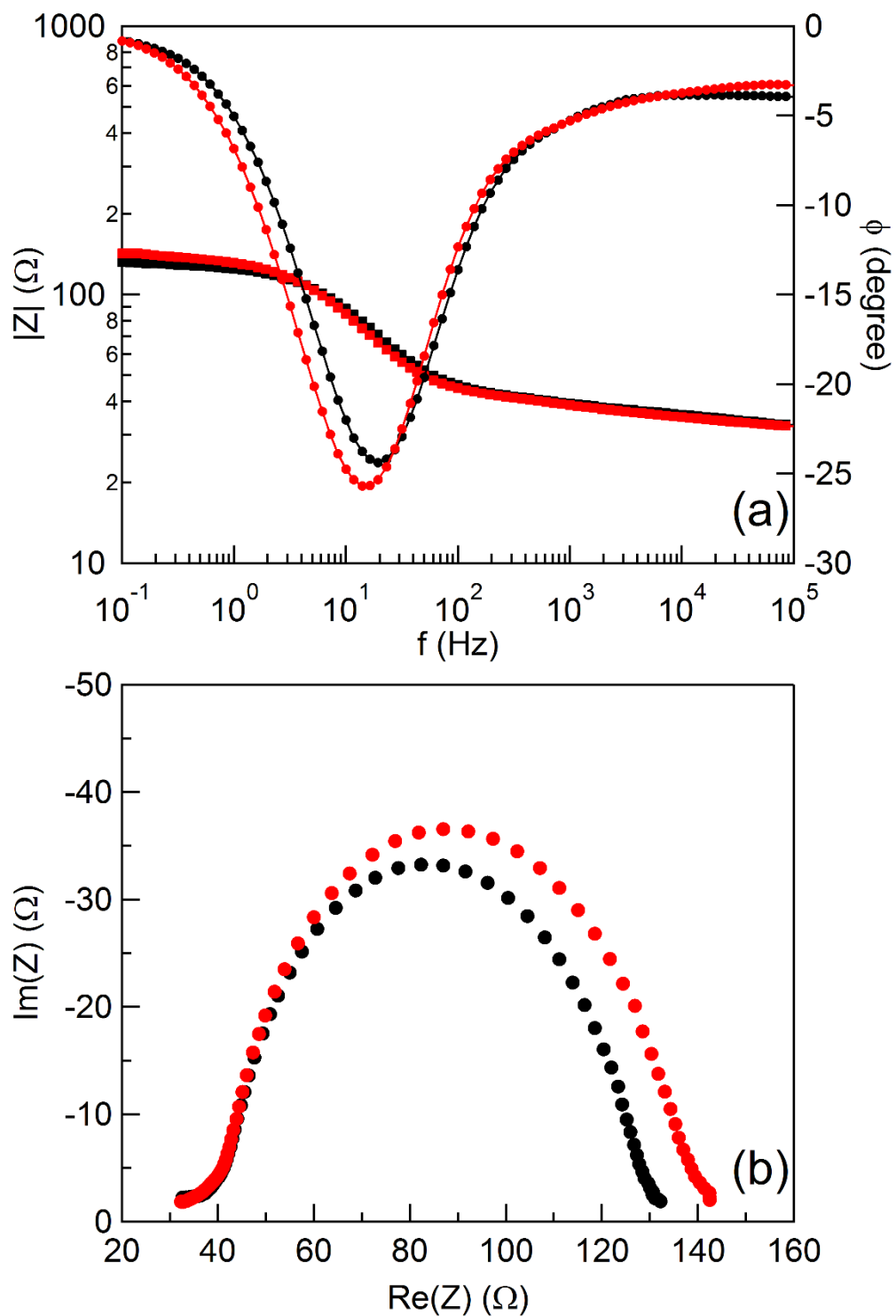
Figure S13. Bode (a) and Nyquist (b) plots of Ni-S/FTO before (black) and after (red) the 1-h electrolysis shown in Figure S9.
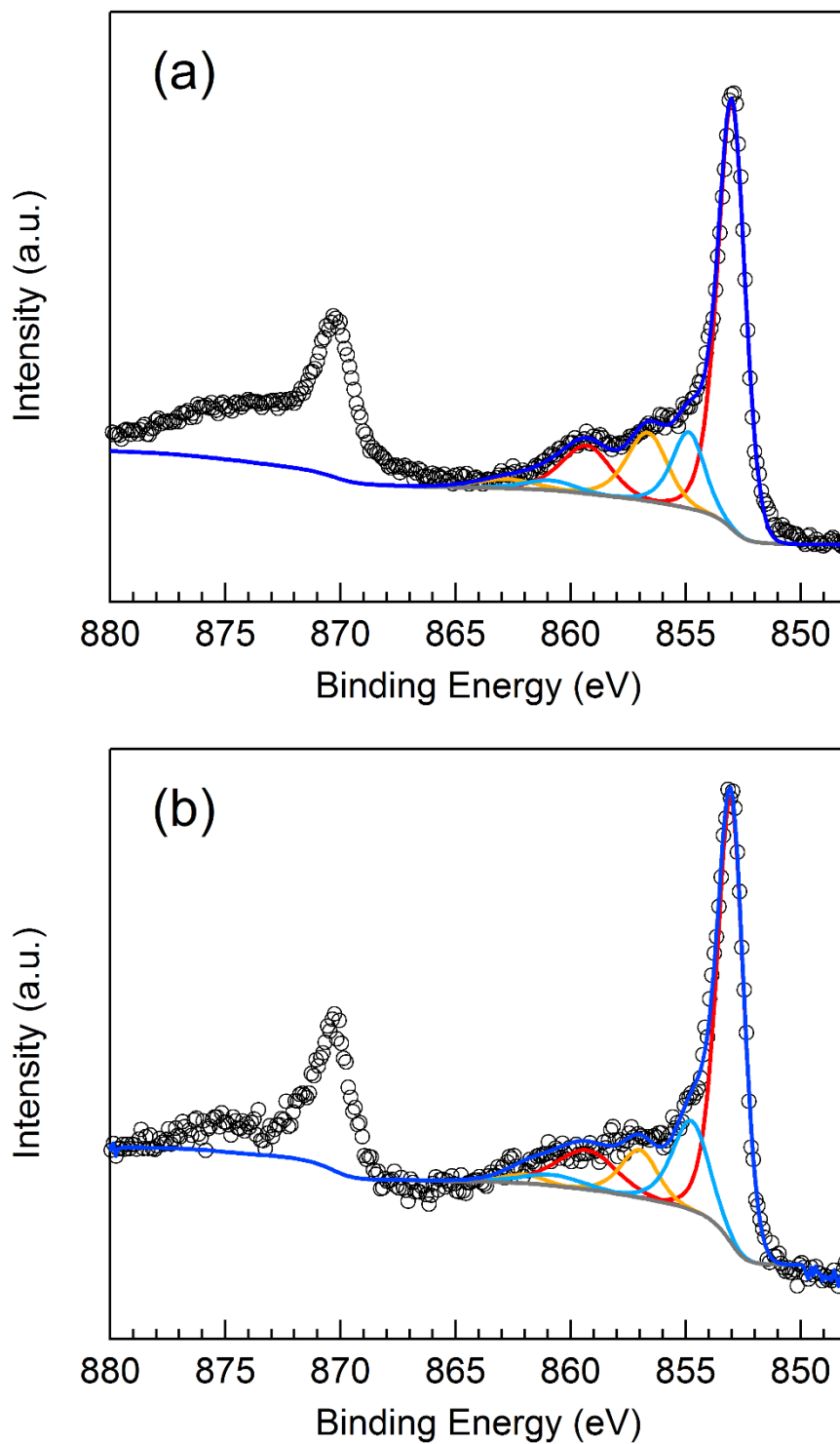
Figure S14. XPS fitting of Ni 2p of Ni-S/FTO before (a) and after (b) the 1-h electrolysis.
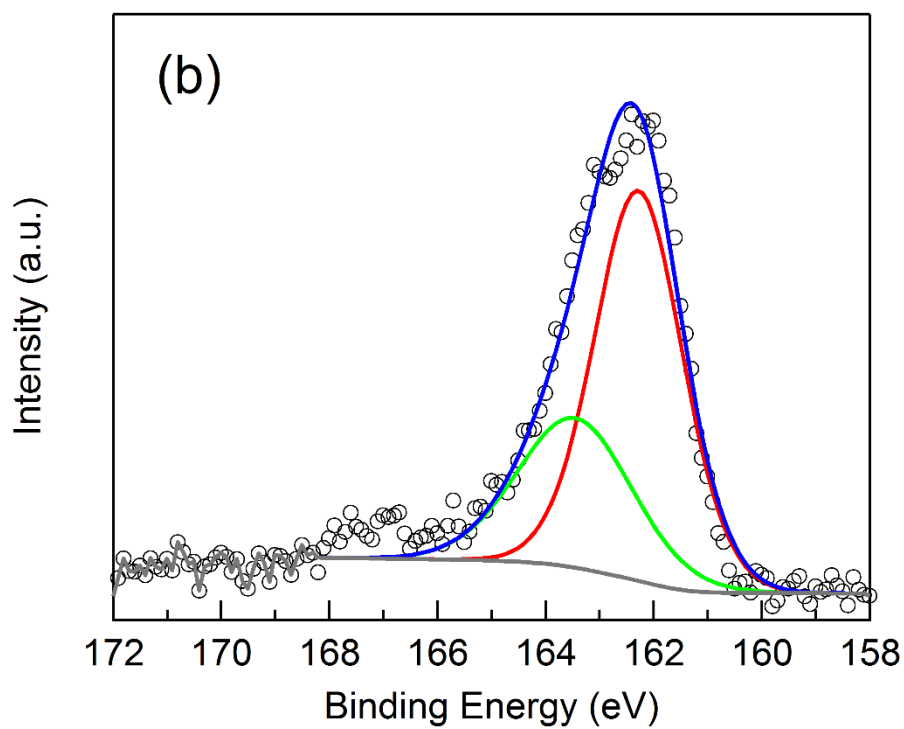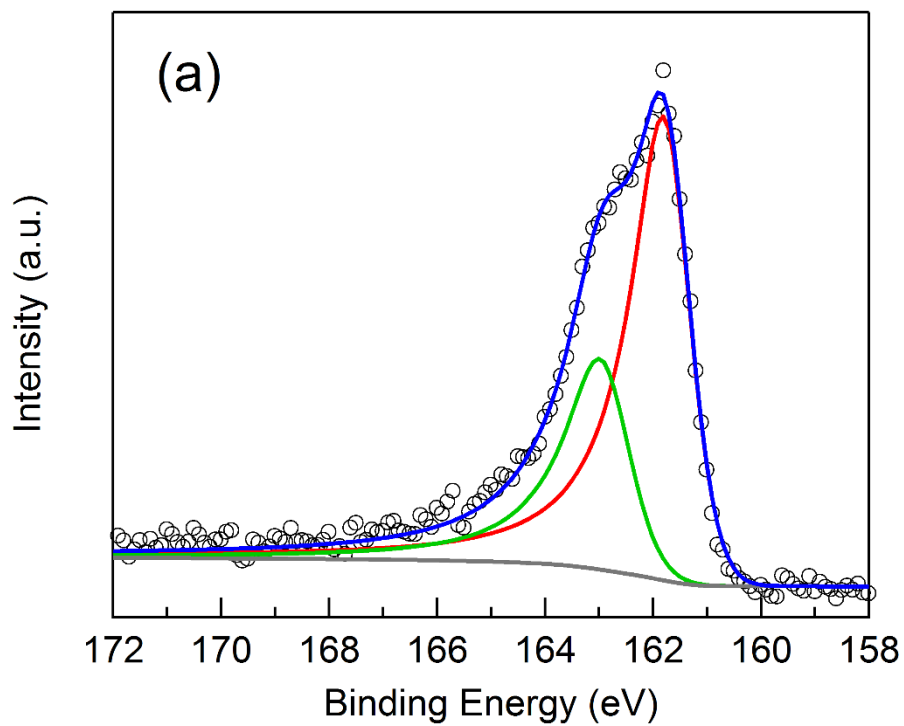
Figure S15. XPS fitting of S 2p of Ni-S/FTO before (a) and after (b) the 1-h electrolysis.
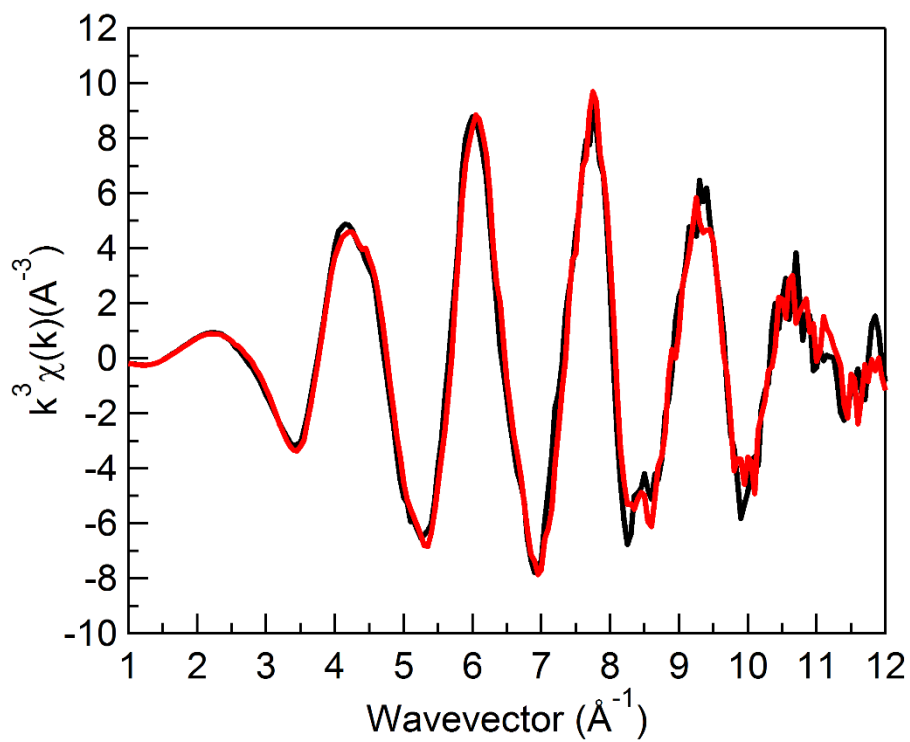
Figure 16. k^3-weighted EXAFS spectra of Ni-S/FTO before (black) and after (red) the 1-h electrolysis.

XAS data analysis

Ni EXAFS Curve Fitting   XAS data fitting was performed with Artemis and IFEFFIT software using ab initio-calculated phases and amplitudes from the program FEFF 8.2.[1,2] These *ab initio* phases and amplitudes were used in the EXAFS equation:

$$\chi(k) = S_0^2 \sum_j \frac{N_j}{kR_j^2} f_{eff_j}(\pi,k,R_j) e^{-2\sigma_j^2 k^2} e^{\frac{-2R_j}{\lambda_j(k)}} \sin(2kR_j + \phi_{ij}(k))$$

The neighboring atoms to the central atom(s) are divided into j shells, with all atoms with the same atomic number and distance from the central atom grouped into a single shell. Within each shell, the coordination number N_j denotes the number of neighboring atoms in shell j at a distance of R_j from the central atom. $f_{eff_j}(\pi,k,R_j)$ is the *ab initio* amplitude function for shell j, and the Debye-Waller term $e^{-2\sigma_j^2 k^2}$ accounts for damping due to static and thermal disorder in absorber-backscatterer distances. The mean free path term $e^{-2R_j/\lambda_j(k)}$ reflects losses due to inelastic scattering, where $\lambda_j(k)$ is the electron mean free path. The oscillations in the EXAFS spectrum are reflected in the sinusoidal term, *sin(2kR_j + $\phi_{ij}(k)$)* where $\phi_{ij}(k)$ is the *ab initio* phase function for shell j. S_0^2 is an amplitude reduction factor due to shake-up/shake-off processes at the central atom(s). The EXAFS equation was used to fit the experimental data using N, R, and the EXAFS Debye-Waller factor (σ^2) as variable parameters. For the energy (eV) to wave vector (k, $Å^{-1}$) axis conversion, E_0 was defined as 8340 eV. The fitting parameters are summarized in Table S4. For the EXAFS curve fitting of the post-electrolysis sample, four cases were considered: (Fit#1) $Ni(OH)_2$ plus Ni_3S_2, (Fit#2) Ni_3S_2 only, (Fit#3) $Ni(OH)_2$ plus NiS_2, and (Fit#4) NiS_2 only. Among those, the best fit was observed when we assume $Ni(OH)_2$ and Ni_3S_2 mixture with $Ni(OH)_2$ as a minority fraction (Fit#1).

Table S4. Ni EXAFS curve fitting parameters of the post-electrolysis film.

Fit	NiO_x:NiS_x		path	R (Å)	N	σ² (Å²)	R (%)
1	Ni(OH)_2	0.08 (0.10)	NiO	2.03 (0.03)	**6**	0.015 (0.005)	7.5 ΔE=-4.1
			NiNi	3.08 (0.05)	**6**	0.003 (0.005)	
	Ni_3S_2	0.92 (0.10)	NiS	2.27 (0.04)	**4**	0.007 (0.002)	
			NiNi	2.51 (0.04)	**4**	0.009 (0.002)	
			NiNi	3.76 (0.11)	**8**	0.023 (0.018)	
			NiNi	4.04 (0.06)	**6**	0.011 (0.004)	
2	Ni_3S_2	1	NiS	2.24 (0.04)	**4**	0.009 (0.002)	8.7 ΔE=-9.9
			NiNi	2.48 (0.03)	**4**	0.008 (0.001)	
			NiNi	3.78 (0.12)	**8**	0.025 (0.016)	
			NiNi	4.00 (0.05)	**6**	0.011 (0.003)	
3	Ni(OH)_2	0.11 (0.12)	NiO	2.03 (0.02)	**6**	0.002 (0.001)	13.4 ΔE=5.0
			NiNi	3.14 (0.04)	**6**	0.003 (0.005)	
	NiS_2	0.89 (0.12)	NiS	2.32 (0.01)	**6**	0.006 (0.001)	
			NiS	3.53 (0.08)	**6**	0.014 (0.012)	
			NiNi	4.12 (0.05)	**12**	0.017 (0.006)	
4	NiS_2	1	NiS	2.32 (0.01)	**6**	0.007 (0.001)	12.7 ΔE=5.0
			NiS	3.37 (0.31)	**6**	0.039 (0.058)	
			NiNi	4.13 (0.04)	**12**	0.018 (0.006)	

S_0 was fixed to 0.83. N is the coordination number and σ^2 is the Debye-Waller factor. ΔE is the EXAFS threshold energy. R factor (%) indicates the goodness of the fit. Bold letters are the fixed parameters. Values in parentheses indicate uncertainties.

References

1. M. Newville, *J. Synchrotron Rad.*, 2001, **8**, 322-324.
2. R. J. J. and A. R. C., *Rev. Mod. Phys.*, 2000, **72**, 621-654.